Progress In Electromagnetics Research B, Vol. 23, 199–214, 2010

STRONG MAGNETIC FIELD INDUCED SEGREGATION AND SELF-ASSEMBLY OF MICROMETER SIZED NON-MAGNETIC PARTICLES

Z. Sun, M. Guo, J. Vleugels, O. van der Biest and B. Blanpain

Department of Metallurgy and Materials Engineering
Katholieke Universiteit Leuven
Kasteelpark Arenberg 44, Bus 2450, Heverlee
Leuven BE-3001, Belgium

Abstract—Micrometer and sub-micrometer sized non-magnetic particles were manipulated by an external strong magnetic field (e.g., 10 Tesla) with a high gradient. During the strong magnetic field effects, segregation of the non-magnetic particles was observed which could not be realised only with gravitational field. Numerical calculations were subsequently carried out to understand the effects on the insulating particles in a conductive liquid matrix. The migration of micrometer sized particles is obviously enhanced by the magnetic field gradient. Combining the experimental results and theoretical analysis, particle-particle magnetic interaction was found to influence the overall segregation of the particles as well. Magnetised by the strong magnetic field, magnetic interaction between non-magnetic particles becomes dominant and a self-assembly behavior can be demonstrated. Various factors such as the magnetic dipole-dipole interaction and chain-chain interaction, are governing the particles assembly. According to calculations, magnetic field should be strong enough, at least 7 T in order to obtain the assembly morphologies in the present case.

1. INTRODUCTION

The use of strong magnetic fields with or without a high gradient is being employed in the field of materials science and engineering [1]. The recent progress is due to the development of superconducting

Received 21 June 2010, Accepted 14 July 2010, Scheduled 22 July 2010
Corresponding author: Z. Sun (zhisun@126.com).

technology which makes strong magnetic fields of 10 T or higher easily attainable [2]. A lot of interesting phenomena have been observed and attracted considerable attention in the field of materials processing. Aspects that have been investigated include magnetic orientation [3], magneto-thermodynamics [4], magneto-hydrodynamics [5] and magnetic effect on chemical reactions [6]. More particularly, the treatment of materials containing particles is a favoured topic. The controllable behavior of small non-magnetic particles using strong magnetic fields — e.g., anisotropic materials preparation [1, 7] and millimeter sized particles assembly [8] — has been of great interest. Although such materials normally show little response to ordinary magnetic fields, e.g., < 1 Tesla, strong magnetic fields, e.g., 10 Tesla can induce efficient magnetic responses from non-magnetic materials [9]. In this case, strong magnetic fields provide an opportunity to control small non-magnetic particle behavior during material preparation.

Unlike ferromagnetic or super-paramagnetic materials, non-magnetic particles especially diamagnetic materials are lack of a permanent magnetic moment. Their magnetisation is directly from the induction of an external magnetic field [10]. Therefore, less agglomeration presents for these materials when compared with magnetic materials, such as magnetic nanoparticles [11], which will be one of the advantages for future applications. In earlier reports, much attention was paid to organic materials such as aromatic peptide [12] and liquid crystal [13] or carbon nanotubes [14] in that these materials are inherent relatively high absolute magnetic susceptibility values. Based on the theories of magnetic energy [15] and magnetic interaction [11, 16], the higher the magnetic susceptibility value is, the stronger the magnetic response will be. On the other hand, the interaction between the particle and the surrounding liquid is believed to play an important role as well during the interparticle magnetic interaction [16–18]. An additional magnetic force which is defined as MHD interaction force is induced when the particle is moving in a conductive liquid [17, 18]. The force is highly depending on the flow field around the particles. In creeping flow region, MHD interaction force is repulsive for sub-micrometer sized particles [17]. However, it can be an attractive force when the flow field becomes more complex and this would contribute to form chains together with the magnetic dipole-dipole interaction force [19] when applying a strong magnetic field.

Up to now, limited reports on the strong magnetic interaction behavior of small non-metallic inorganic particles inherent very low magnetic susceptibility values. In the present paper, magnetic

interaction between micrometer sized oxide particles is demonstrated. Magnetic field effects on single particle is discussed and compared with numerical calculations. With a strong enough magnetic field, magnetic interaction behaviors due to the applied magnetic field become dominant and self-assembly of the particles can be realized. To validate the observation, factors such as treatment time and magnetic flux density are examined. In addition, theoretical analysis are performed to discuss the segregation and assembly behavior.

2. EXPERIMENTAL

In order to carry out the experiments and obtain a system of diamagnetic non-metallic particle-conductive liquid, modeling sample of Pb-Sn solder alloy provided by Metallo N. V. with a composition of 26.9 wt% Sn was chosen during the experiments. The alloy contains dissolved oxygen and was covered with an oxide residue layer. The residue was removed and the remaining material was machined into cylindrical samples with a diameter of 9 mm and a height of 12 mm. After sealing the sample with inert refractory materials inside of a tube of high purity corundum, the tube was mounted with a sample holder into a tube furnace which was placed in a vertical strong magnetic field reaching up to 12 T generated by a superconducting magnet. The temperature of the furnace can reach 900 °C and was controlled to a precision of ±1 °C. The experimental apparatus is schematically presented in Fig. 1, together with the magnetic field and gradient distribution. Distributions of the magnetic field along the vertical direction were measured with a magnetic fluxmeter (HT700SP, Shanghai YAHAO). The furnace consisting of non-magnetic materials has negligible influence on the magnetic field distribution. The sample was initially heated to 330 °C and kept for around 30 min to ensure complete melting. The temperature was subsequently cooled to 270 °C (around the liquidus temperature) at a cooling rate of 5 °C/min in order to precipitate oxide phases from the oxygen saturated Pb-Sn melt matrix. After a predefined holding time at 270 °C, the sample was drawn out of the magnet for quenching in water at room temperature. The sample was removed as fast as possible to make sure that the particles did not have enough time to migrate before being frozen. The temperature profile during the experiments is given in Fig. 1(c). The magnetic field is kept as constant in the process of oxide particles generation and interaction.

The cold samples were cut along the longitudinal direction and polished for scanning electron microscopy (Philips XL 30 FEG, the Netherlands) examination and semi-quantitative analysis with an

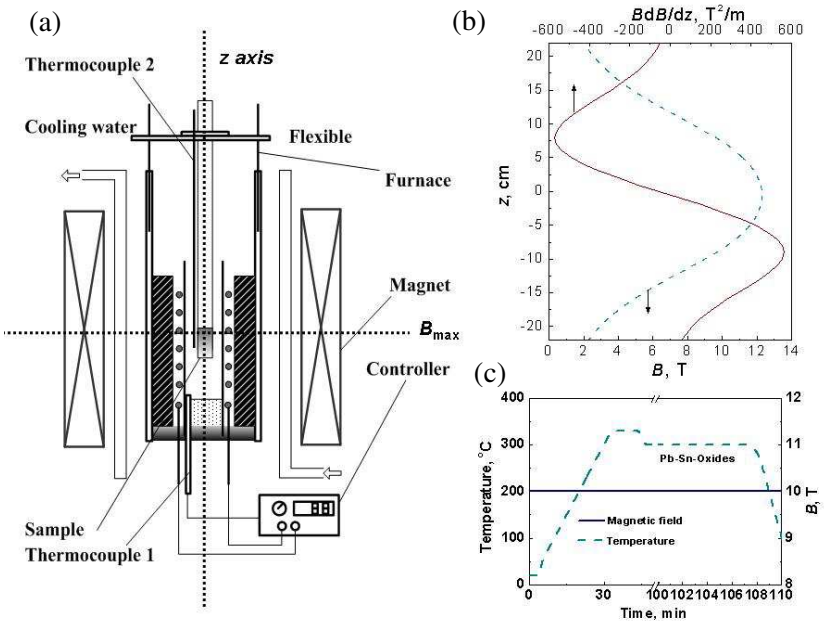

Figure 1. Schematic representation of the experimental apparatus and heating procedures. (a) Experimental resistance furnace in the superconducting magnet; (b) Magnetic field and magnetic field gradient product distribution; (c) Heating procedures during the experiments.

energy dispersive X-ray spectrometer (EDAX, the Netherlands). The macro- and microstructures of the samples with and without the magnetic field treatment were investigated and the compositional gradient as well as the non-metallic particle distribution was obtained. To verify the composition of the oxides, X-ray diffraction (XRD) analyses were carried out of the as-products (XRD, Siemens D500).

3. RESULTS

To understand the effect of the strong magnetic field with a high gradient, the effect of the magnetic flux density and treatment time on the non-magnetic particle (precipitated oxide phase) segregation was investigated. Fig. 2 gives a comparison of the oxygen content distribution through the sample axial cross-section which indicates the oxide particle distributions with and without magnetic field treatment.

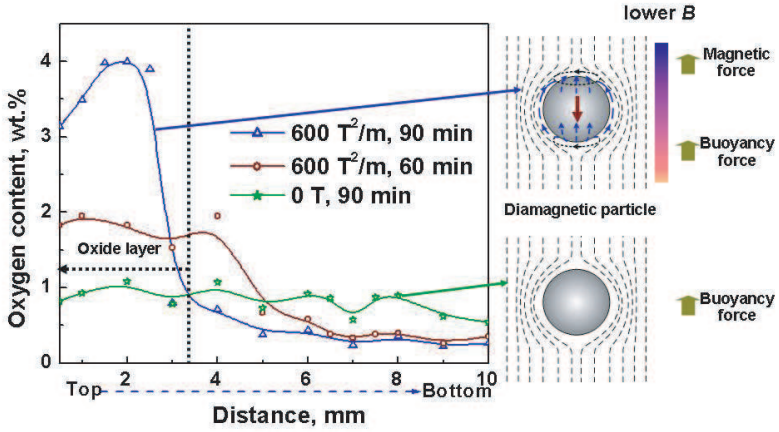

Figure 2. Effect of the strong magnetic field gradient on the oxygen distribution along the cross-sectioned cylindrical samples with or without the magnetic field treatment. Without magnetic field, a single particle gets only the buoyancy force because of the density difference; when a gradient magnetic field is applied, magnetic force/magnetic Faraday force works on the diamagnetic particle as well.

It is easily detected that, the migration depends significantly on the gradient product ($B\mathrm{d}B/dz$, Fig. 1(b)) and the holding time (Fig. 2). When segregation is observed, an obvious transit point exists where the oxygen content changes from a very low value to a high value (Fig. 2). The oxide layer thickness is then defined as the distance from the transit point to the "Top" (Fig. 2). According to Fig. 2, the oxide layer becomes thinner with longer magnetic field treatment time, indicating an enhanced segregation. No obvious migration can be found when the gradient magnetic field is absent.

Figure 3 illustrates a comparison of the non-magnetic particles interaction behaviors with and without a strong magnetic field treatment. Non-magnetic particles distribute randomly when the magnetic field is absent (Figs. 3(a1) and (a2)) and particle chains can be formed when applying a strong enough magnetic field, indicating an obvious magnetic interaction (Figs. 3(b1) and (b2)). According to EDAX analysis, the oxide particle (black phase in the backscattered electron image) in Fig. 3 is SnO_2 doped with some amount of PbO_2 (around 20 at %). This is confirmed as well by X-ray diffraction analysis of the whole sample. Nevertheless, the particles precipitated inside and outside of the magnetic field exhibit fairly

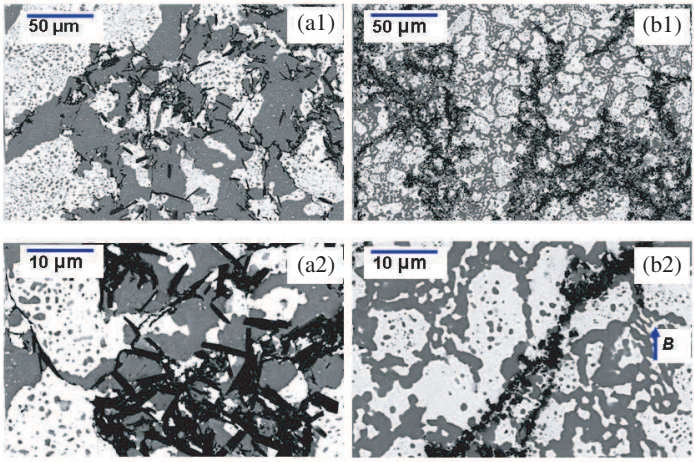

Figure 3. Effect of strong magnetic field with a high gradient on the segregation and self-assembly of the non-metallic particles. The SEM backscattered electron images, (a1) and (a2) are the SEM-BSE images of the sample treated without a magnetic field; (b1) and (b2) are the images of the sample treated with a strong magnetic field. Note: black phase: oxide particle; white phase: Pb; gray phase: $PbSn_2$.

distinctive morphologies. Based on earlier researches, a shift of phase transformation and crystal morphologies induced by a strong magnetic field has been already realised [4]. The results now clearly indicate that, the nature of the precipitated phase can also be influenced by the magnetic field. The reason is believed to be that the oxygen transfer as well as the flow of the liquid melt is slowed down by the strong magnetic field [20]. The gray matrix in all images of Fig. 3 is identified as a phase with composition of eutectic phase with a small amount of dissolved oxygen. In the matrix, the white phase which is finer in Figs. 3(a) and (b) is Pb. The exact phase analysis is beyond the scope of this paper since the main focus is on the influence of the magnetic field on the oxide particles interaction. The lack of detailed information of the influence of strong magnetic fields on Pb-Sn-O phase diagram and impurities in the alloy would also make the analysis more complex.

4. DISCUSSION

4.1. Strong Magnetic Field Induced Non-magnetic Particles Segregation

The induced migration of the non-magnetic oxide particles is due to the additional magnetic Faraday force (Equation (1)). During strong magnetic field treatment, the samples were put in the position with the highest gradient product ($B\mathrm{d}B/dz$) where the Faraday force is in the same direction as the buoyancy force (Equation (2)).

$$F_B = V(\chi_M - \chi_P)\frac{1}{\mu_0}B\frac{dB}{dz} \tag{1}$$

where $\mu_0(= 4\pi \times 10^{-7}\,\mathrm{Hm}^{-1})$ is the magnetic permeability of the vacuum, χ_M and χ_P are, respectively, the volumetric mass magnetic susceptibility of the melt and the diamagnetic oxide particle, V is the volume of the particle.

Under low magnetic fields, the feeble magnetic non-metallic particle itself is subjected to a weak magnetic force and the migration is negligible [8]. However, when a large difference of the magnetic susceptibility between the particle and the matrix exists, migration of the magnetised particles can be significantly enhanced especially for micrometer-sized particles [21]. This is a prerequisite to induce significant migration of the non-magnetic particles using a strong magnetic field. In our case, the magnetic susceptibilities of the non-metallic SnO_2 of -2.38×10^{-5} and PbO_2 of -1.29×10^{-5} are much smaller than the liquid metal matrix $PbSn_2$ (eutectic phase) of 1.90×10^{-6} according to reference [22] which are shown in Table 1. When the magnetic field is absent, the particles disperse in the matrix without any macro segregation. The current experiments however reveal that non-metallic particles are collected to one side of the sample and the segregation layer becomes thinner with the increase of the treatment time (Fig. 2) when strong magnetic fields with a high gradient are employed.

Together with the magnetic Faraday force, buoyancy force F_g acts as a driving force for the non-magnetic particles segregation.

$$F_g = V(\rho_M - \rho_P)g \tag{2}$$

where ρ_M and ρ_P are the densities of the liquid melt and of the non-metallic inclusion, respectively, g is the gravitational acceleration.

With only the gravitational field, no obvious segregation of the non-metallic particles was observed, as shown in Fig. 2, implying that the buoyancy force is so insignificant. In the present case, the magnetic Faraday force is around two times of the buoyancy force based on the

Table 1. Physical properties of materials considered in the present case.

Physical properties	SnO_2	PbO_2	$PbSn_2$
Density, ρ, kg/m^3	6950	9380	8300 (liquid)
Magnetic susceptibility, χ, (SI, volume)	-2.38×10^{-5}	-1.29×10^{-5}	1.90×10^{-6}
Viscosity, η, Pa·s	–	–	2.5×10^{-3}
Electrical conductivity, σ, $(\Omega \cdot \mathrm{m})^{-1}$	–	–	1.3×10^{6}

data in Table 1. This observation also indicates a substantial that the magnetic Faraday force is considerable and the magnetic force plays a key role in the formation of gradient particle distribution. At the same time, a single non-metallic particle experiences the Stokes viscosity force during migration. The drag force can be expressed by Equation (3).

$$F_{\eta,B} = 3\pi\eta_{M,B}v_P d_P \tag{3}$$

where $F_{\eta,B}$ is the Stokes viscosity drag force (for spherical particle with Reynolds number less than 1), $\eta_{M,B}$ is the viscosity of the liquid in strong magnetic field; v_P is the inclusion velocity and d_P is the diameter.

When a particle is migrating in a conductive liquid, the viscosity performs as a drag on the particle and its value depends on the present conditions, e.g., temperature, pressure. In a strong magnetic field, the interaction behavior and thermodynamics status of the molecules in the liquid will be changed and therefore the viscosity of the conductive liquid is expected to be modified [15]. Experimental results [23, 24] have demonstrated that the magnetic field can increase the viscosity and some experiential equations have already been derived from the measured data describing the magnetic field dependence of the viscosity [23]. According to [16, 22, 25], the magnetic field effect on a conductive liquid viscosity can be derived from the Hartmann number (Ha) [26] according to Equation (4). The viscosity then becomes an effective viscosity $\eta_{M,B}$. It indicates that the drag force and the Faraday force increase simultaneously with increasing the magnetic flux density. Consequently, it becomes the reason for insufficient enhancement of the migration of larger particles under strong magnetic fields [16].

$$\eta_{M,B} \cong \eta_M \left(1 + \frac{1}{3}Ha\right) \tag{4}$$

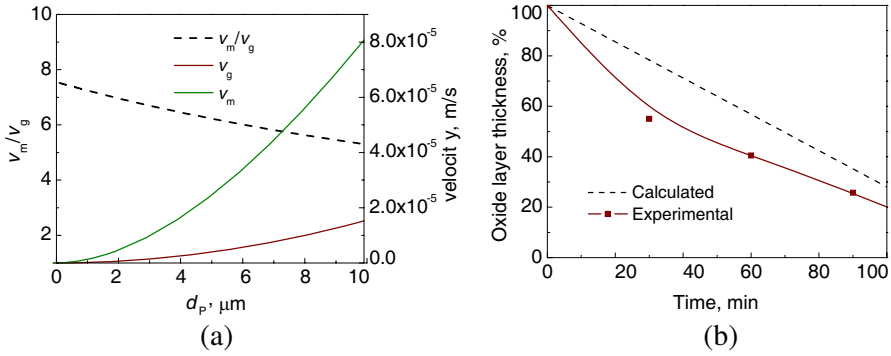

Figure 4. Effect of the strong magnetic field on the particle migration. (a) The maximum migration velocities as a function of the particle size with v_m and without v_g the magnetic field treatment (10 T, 60 T/m); (b) Comparison of calculated oxide layer thickness and the experimental results.

where $Ha = B\frac{d_P}{2}(\frac{\sigma_M}{\eta_M})^{1/2}$ and σ_M is the electrical conductivity of the liquid melt at a certain temperature.

By further assuming that the drag is the only opposing force to the driving forces in axial direction (shown in Fig. 2), the resultant velocities can be evaluated via Newton's second law as a function of the particle size. Here we assume the particle is SnO_2. From the results in Fig. 4, an obvious increase of the particle motion is found in the present case when the particle size is around or less than 2 μm. The particle migration velocity under magnetic field v_m can reach around 7 times of that under gravitational field v_g. To sum up, the distribution of micrometer non-metallic particles can be controlled by combining the above mentioned effects of the strong magnetic field.

Additionally, the oxide layer thickness can be estimated theoretically based on the particle migration velocities in Fig. 4(a). The average diameter 2.0 μm is adopted during the calculation and the oxide thickness layer is converted into percentage of the whole sample length. The oxide layer thickness is calculated from the subtraction of the migrating distance and the length of the sample. The comparison of the calculated oxide layer thickness and the experimental results is shown in Fig. 4(b). A deviation presents that the experimental thickness is smaller than the theoretical estimation. The reason is believed that the magnetic interaction increase the effective diameter of the particle by forming chains or clusters.

4.2. Magnetic Interaction of Non-metallic Particles Induced by Strong Magnetic Fields

Under strong magnetic fields, the feeble magnetic, non-metallic particles can be magnetised and their interaction becomes considerable. Figs. 3 (a1), (a2) and (b1), (b2) illustrate the non-metallic particles (black phase) self-assembly morphologies when the magnetic field is absent and when it is 10 T. In the absence of the magnetic field, the oxide particles are randomly distributed and clustered

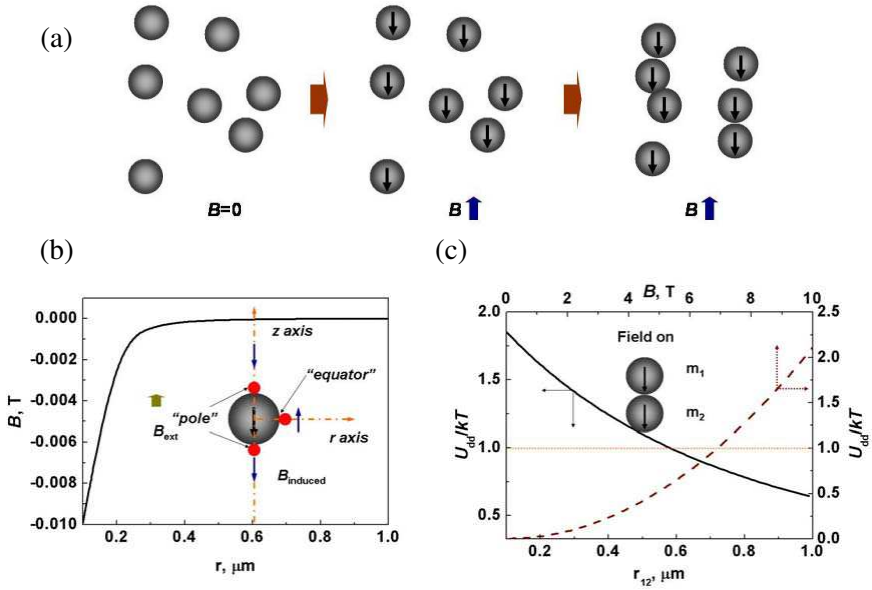

Figure 5. Magnetic interaction of two non-metallic particles. (a) Schematic plot of the assembly process of the non-magnetic particles in a strong magnetic field; (b) Induced magnetic field distribution of a diamagnetic dipole; (c) Comparison of the magnetic dipole-dipole interaction energy and the thermal energy, depending on the particles separation distance and the magnetic field density. The magnetic field density is set as 10 T when considering the particles separation distance effect. The particles separation distance is set as 0 when taking account of the magnetic field density effect. It can be found that the particle separation distance should be smaller than 0.6 μm in order to get an assemble morphology at 10 T magnetic field. The magnetic field density should be at least 7 T in order to observe an obvious interaction behavior between the non-magnetic particles in the present case.

(Figs. 3(a1) and (a2)) and no further self-assembly structures are found. However, chain-like structures, which are formed by a number of non-metallic particles, can be observed after being treated by the strong magnetic field (Figs. 3(b1) and (b2)). This reveals the presence of an interparticle interaction due to the magnetic field. A schematic plot of the assembly process can be shown in Fig. 5(a). Moreover, short chains tend to connect head to tail as there the attractive force is dominant [27]. Whereas the linear structures shown in Fig. 3(b1) are expected to align in the direction of the externally applied magnetic field, branching and deflection do always exist. A possible reason is the steric hindrance of primary lead phase according to the Pb-Sn binary phase diagram. Meanwhile, the lead phase seems acting as a matrix together with the $PbSn_2$ in the present case. Therefore, the disorder also provides additional evidence that the dipole-dipole interactions play an important role to get rid of the hindrance.

The oxide particle inherent a diamagnetic property and the induced magnetic field distribution can be obtained by

$$\vec{B}_{Induced} = \vec{B}_{dipolar} = \frac{\mu_0}{4\pi}\frac{\vec{m}_i\vec{r}}{r^3} \tag{5}$$

where the magnetic moment $\vec{m}_i = V\chi_i B_{ext}/\mu_0\vec{r}$ and r are the unit vector and the distance from the magnetic dipole respectively (here we adopt cylindrical coordinate r, θ, z).

The magnetic field is distorted by $\vec{B}_{Induced}$ and the dipolar magnetic field adds to the external field at the "equator" of the diamagnetic oxide particle. At the same time, the dipolar magnetic field subtracts the external magnetic field at the "pole" position (Fig. 5(b)). Here we assume the external static magnetic field has a constant magnetic field gradient 600 T/m throughout the whole sample and therefore the magnetic field deviation in a step size of 2 µm (particle diameter) is 1.2×10^{-3} T. The one dimensional induced magnetic field distribution along z-axis can be calculated according to Equation (5) and shown in Fig. 5(b). It can be found that, the induced magnetic field is around 10^{-2} T near to the particle. In a local inhomogeneous magnetic field, the magneto-static potential energy of a point dipole is expressed as

$$U_i = -V\chi_P\frac{1}{\mu_0}(B_{local})^2 \tag{6}$$

where B_{local} is the local magnetic field including the externally applied and induced magnetic field.

For diamagnetic particles, the magneto-static potential energy is positive and thus a particle is driven to the "pole" of another diamagnetic particle when they are approaching.

Subsequently the interaction between two dipoles can be described by the dipole-dipole interaction energy U_{dd}. In a strong magnetic field, U_{dd} between particles 1 and 2, presented in Fig. 5(c), can be expressed as [11]

$$U_{dd} = \frac{\mu_0(1+\chi_M)}{4\pi r_{12}^3}\left[(\mathbf{m}_1 \cdot \mathbf{m}_2) - 3\,(\mathbf{m}_1 \cdot \mathbf{e}_{12})\,(\mathbf{m}_2 \cdot \mathbf{e}_{12})\right] \tag{7}$$

where $\mathbf{m}_1$, $\mathbf{m}_2$ are the magnetic dipoles, r_{12} is the dipole-dipole distance and $\mathbf{e}_{12}$ is the unit vector parallel to the line joining the centers of the two dipoles.

When two particles assemble in a head-to-tail configuration along with the external magnetic field ($\mathbf{e}_{12}$ paralleling with B, Fig. 5(c)) due to the magneto-static potential energy, the second part in Equation (7) is $3\mathbf{m}_1\mathbf{m}_2$ and U_{dd} is negative. It means the two particles will attract each other to reduce the magnetic interaction energy. In a magnetic field of 10 T, the magnitude of the interaction force can reach the value of the gravity force especially for smaller particles or clusters [17].

Besides of the migration of the particles is influenced by their magnetic interaction, the interaction can also be interfered by the migration. During migration, another kind of interaction force is induced due to the conductive melt flow. The force can be roughly expressed as [16, 17]

$$F_f^{(m)} \propto -\frac{d_P^8 B^2 \sigma_M^2 v_P^2}{l_{12}^4} \tag{8}$$

where σ_M is the electrical conductivity of the melt. $F_f^{(m)}$ acts as a repulsive force, weakening the dipole-dipole attractive force of two non-metallic particles. However, it has very small magnitudes in creeping flow regime and highly depends on the fluid flow [17]. For more complex fluid flow, the force can function as an attractive interaction force. A detailed investigation can be found elsewhere [19].

In addition to the interparticle forces, chain-chain interaction exists as related to the dipole-dipole interaction, governing the chain-coarsening perpendicular to the magnetic field. According to the literatures [27, 28], the lateral aggregation or coarsening can only be evoked in a rather high particle concentration due to collision or energy decline. The aggregation is usually observed at the end of the chains since the potential energy for the particle located near the end of a chain is much lower [3, 5]. In our case, this kind of interaction seems much more pronounced as shown in Figs. 3(b1) and (b2) where chain-like structures become connected and even interlaced. A reason is the divergence of particle size and the aligning process of each particle to the preferred magnetisation direction due to its anisotropic magnetic

property. In addition, the segregation of the particles induced by the gradient magnetic field makes the local conditions more complex and the collision probability increases. Moreover, the competition with Brownian motion may disturb the particles alignment as well. Another factor is that the particles are migrating during the formation of chains. Therefore, the particle size and its precipitated location can also change the self-assembly structures. Consequently, a web-like structure is assembled.

5. CONCLUSIONS

In the present paper, the segregation and interaction behavior of micrometer sized non-magnetic particles is investigated using strong magnetic fields with high gradient. A conclusion can be drawn as follows:

1) Non-metallic particles are collected into one side of the sample when the strong magnetic fields with high gradient are employed and the thickness of the segregation layer significantly depends on the gradient product ($B\mathrm{d}B/dz$) and treatment time. The migration is dominated by the driving force (the Buoyancy force and the Faraday force) and the drag force. The Faraday force and the viscosity drag force are both increased with the magnetic field, indicating a counteracting behavior. Combining the effects of the magnetic field, the distribution of non-metallic particles can be easily controlled.
2) The self-assembly structures of the non-metallic particles are governed by the magnetic dipole-dipole interaction force. The dipole-dipole attractive force in the perpendicular orientation and the repulsive force induced by the flow of the melt determine the head-to-tail morphology while the dipole-dipole repulsive force in parallel orientation and the chain-chain interaction determine the coarsening of the chain-like structures. Influenced by a variety of factors, a web-like self-assembly morphology is formed.

In addition, it proves that small non-metallic particles can be manipulated and controlled by imposing an external strong magnetic field and provides a new possibility of strong magnetic fields application.

ACKNOWLEDGMENT

Financial support from of the Flemish Institute for the Promotion of Scientific Technological Research in Industry (IWT) under contract

SBO-PROMAG (60056) is gratefully acknowledged. The authors acknowledge Dr. Bert Coletti from Metallo N. V. for providing the alloy materials. The group of Prof. Zhongming Ren in Shanghai University is acknowledged for all the kind help during the experiments.

REFERENCES

1. Asai, S., K. Sassa, and M. Tahashi, "Crystal orientation of non-magnetic materials by imposition of a high magnetic field," *Science and Technology of Advanced Materials*, Vol. 4, 455–460, 2003.
2. Motokawa, M., "Physics in high magnetic fields," *Rep. Prog. Phys.*, Vol. 67, 1995–2052, 2004.
3. Hangarter, C. M., Y. Rheem, B. Yoo, E. Yang, and N. V. Myung, "Hierarchical magnetic assembly of nanowires," *Nanotechnology*, Vol. 18, 205305, 2007.
4. Ren, Z., X. Li, Y. Sun, Y. Gao, K. Deng, and Y. Zhong, "Influence of high magnetic field on peritectic transformation during solidification of Bi-Mn alloy," *Calphad*, Vol. 30, 277–285, 2006.
5. Reitz, J. R. and F. J. Milford, *Foundations of Electromagnetic Theory*, Addison-Wesley Publishing Company, London, England, 1962.
6. Larachi, F. and M. C. Munteanu, "Magnetic emulation of microgravity for earth-bound multiphase catalytic reactor studies Potentialities and limitations," *AIChE J.*, Vol. 55, 1200–1216, 2009.
7. Sun, Z., L. Zhang, M. Guo, J. Vleugels, O. van der Biest, and B. Blanpain, "Non-magnetic anisotropic-materials preparation by a strong magnetic field during the solidification of a hypereutectic Al-Cu alloy," *EPL*, Vol. 89, 64002, 2010.
8. Takayama, T., Y. Ikezoe, H. Uetake, N. Hirota, and K. Kitazawa, "Self-organization of nonmagnetic spheres by magnetic field," *Appl. Phys. Lett.*, Vol. 86, 234103–234103, 2005.
9. Berry, M. V. and A. K. Geim, "Of flying frogs and levitrons," *Eur. J. Phys.*, Vol. 18, 307–313, 1997.
10. Crangle, J., *The Magnetic Properties of Solids*, Edwad Arnold Limited, London, 1977.
11. Bishop, K. J. M., C. E. Wilmer, S. Soh, and B. A. Grzybowski, "Nanoscale forces and their uses in self-assembly," *Small*, Vol. 5, 1600–1630, 2009.

12. Hill, R. J. A., V. L. Sedman, S. Allen, P. Williams, M. Paoli, L. Adler-Abramovich, E. Gazit, L. Eaves, and S. J. B. Tendler, "Alignment of aromatic peptide tubes in strong magnetic fields," *Advanced Materials*, Vol. 19, 4474–4479, 2007.
13. Boamfa, M. I., S. V. Lazarenko, E. C. M. Vermolen, A. Kirilyuk, and T. Rasing, "Magnetic field alignment of liquid crystals for fast display applications," *Advanced Materials*, Vol. 17, 610–614, 2005.
14. Garmestani, H., M. S. Al-Haik, K. Dahmen, R. Tannenbaum, D. Li, S. S. Sablin, and M. Y. Hussaini, "Polymer-mediated alignment of carbon nanotubes under high magnetic fields," *Advanced Materials*, Vol. 15, 1918–1921, 2003.
15. Yamaguchi, M. and Y. Tanimoto, *Magneto-science (Magnetic Field Effects on Materials: Fundamentals and Applications)*, Springer-Verlag, Berlin, Heidelberg, New York, 2006.
16. Sun, Z., M. Guo, F. Verhaeghe, J. Vleugels, O. van der Biest, and B. Blanpain, "Magnetic interaction between two non-magnetic particles migrating in a conductive fluid induced by a strong magnetic field-an analytical approach," *Progress In Electromagnetics Research*, Vol. 103, 1–16, 2010.
17. Sun, Z., T. Kokalj, M. Guo, F. Verhaeghe, O. van der Biest, B. Blanpain, and K. van Reusel, "Effect of the strong magnetic field on the magnetic interaction between two non-magnetic particles migrating in a conductive fluid," *EPL*, Vol. 85, 14002, 2009.
18. Chester, W., "The effect of a magnetic field on stokes flow in a conducting fluid," *Journal of Fluid Mechanics*, Vol. 3, 304–308, 1957.
19. Sun, Z., M. Guo, J. Vleugels, O. van der Biest, and B. Blanpain, "Numerical simulations of the 'strong magnetic field effects' on micrometer sized insulating (inert) particle(s) moving in a conductive fluid," *Physical Review E*, submitted, 2010.
20. Maki, S., M. Ataka, T. Tagawa, and H. Ozoe, "Natural convection of a paramagnetic liquid controlled by magnetization force," *AIChE J.*, Vol. 51, 1096–1103, 2005.
21. Sun, Z., M. Guo, J. Vleugels, O. van der Biest, and B. Blanpain, "Numerical calculations on inclusion removal from liquid metals under strong magnetic fields," *Progress In Electromagnetics Research*, Vol. 98, 359–373, 2009.
22. Weast, R. C., M. J. Astle, and W. H. Beyer, *CRC handbook of Chemistry and Physics*, CRC Press, Inc., Florida, USA, 1983–1984.

23. Sun, C., H. Geng, N. Zhang, X. Teng, and L. Ji, "Viscous feature of Sb-Bi alloy under magnetic field," *Materials Letters*, Vol. 62, 73–76, 2008.
24. Ghauri, S. and M. Ansari, "Increase of water viscosity under the influence of magnetic field," *Journal of Applied Physics*, Vol. 100, 066101–066102, 2006.
25. Yasuda, H., I. Ohnaka, O. Kawakami, K. Ueno, and K. Kishio, "Effect of magnetic field on solidification in Cu-Pb monotectic alloys," *ISIJ Inter.*, Vol. 43, 942–949, 2003.
26. Davidson, P. A., *An introduction to Magnetohydrodynamics*, Cambridge University Press, 2001.
27. Butter, K., P. Bomans, P. M. Frederik, G. J. Vroege, and A. P. Philipse, "Direct observation of dipolar chains in iron ferrofluids by cryogenic electron microscopy," *Nat. Mater.*, Vol. 2, 88–91, 2003.
28. Fang, W., Z. He, X. Xu, Z. Mao, and H. Shen, "Magnetic-field-induced chain-like assembly structures of Fe_3O_4 nanoparticles," *EPL*, Vol. 77, 68004, 2007.